The role of the superficial region in determining the dynamic properties of articular cartilage

Alanna R. Gannon[1], Thomas Nagel[1, 2] & Daniel J. Kelly[1]

[1]Trinity Centre for Bioengineering, School of Engineering, Trinity College Dublin, Dublin, Ireland

[2]Department of Environmental Informatics, Helmholtz Centre for Environmental Research GmbH – UFZ, Permoserstraße 15, 04318 Leipzig, Germany

Address correspondence to:

Dr. Daniel Kelly
Trinity Centre for Bioengineering
Department of Mechanical Engineering
Parsons Building
Trinity College Dublin
Dublin 2
Ireland

Tel: +353.1.896.3947

Fax: +353.1.679.5554

Email: kellyd9@tcd.ie

Original article submitted to: Osteoarthritis and Cartilage

First submitted: March 2012

Resubmitted: June 2012

Resubmitted: July 2012

Total word count: 3999

Keywords: Articular cartilage, superficial tangential zone, dynamic loading, biomechanics, osteoarthritis.

Abstract

Objective: The objective of this study was to elucidate the role of the superficial region of articular cartilage in determining the dynamic properties of the tissue. It is hypothesised that removal of the superficial region will influence both the flow dependent and independent properties of articular cartilage, leading to a reduction in the dynamic modulus of the tissue.

Methods: Osteochondral cores from the femoropatellar groove of three porcine knee joints were subjected to static and dynamic loading in confined or unconfined compression at increasing strain increments with and without their superficial regions. Equilibrium moduli and dynamic moduli were measured and the tissue permeability was estimated by fitting experimental data to a biphasic model.

Results: Biochemical analysis confirmed a zonal gradient in the tissue composition and organisation. Histological and PLM analysis demonstrated intense collagen staining in the superficial region of the tissue with alignment of the collagen fibres parallel to the articular surface. Mechanical testing revealed that the superficial region is less stiff than the remainder of the tissue in compression, however removal of this region from intact cores was found to significantly reduce the dynamic modulus of the remaining tissue, suggesting decreased fluid load support within the tissue during transient loading upon removal of the superficial region. Data fits to a biphasic model revealed a significantly lower permeability in the superficial region compared to the remainder of the tissue.

Conclusions: It is postulated that the observed decrease in the dynamic moduli is due at least in part to the superficial region acting as a low permeability barrier, where its removal decreases the tissue's ability to maintain fluid load support. This result emphasises the impact that degeneration of the superficial region has on the functionality of the remaining tissue.

1. Introduction

Articular cartilage is a thin layer of highly specialized tissue that functions to support and redistribute joint contact forces and to reduce friction within the joint. It is comprised of a specialised cell type; chondrocytes, embedded in an abundant fluid filled extra-cellular matrix (ECM) that consists mainly of a collagen type II network containing water and the large aggregating proteoglycan aggrecan, the latter of which consists of a protein core to which numerous negatively charged glycosaminoglycan (GAG) side chains are attached [1-3]. Articular cartilage demonstrates a depth dependent heterogeneous composition and ultra-structure, traditionally divided into three distinct zones. Each zone has a distinct ECM composition, organisation and cell morphology, with the shape and arrangement of the chondrocytes in these zones believed to be related to the local architecture of the collagen fibrils within the solid matrix [4]. In the superficial tangential zone (STZ) collagen fibres are densely packed and orientated parallel to the articular surface while the proteoglycan content is lowest. In the middle zone (MZ) the collagen fibres are larger, less dense and arcade from a parallel to a perpendicular orientation resulting in a more random organisation. The concentration of PG aggregates increases with depth from the articular surface negatively correlating to decreases in water content and thus resulting in higher swelling pressures with tissue depth [5]. Finally in the deep zone collagen fibres are arranged perpendicular to the subchondral bone thus anchoring the tissue to its bony bed [6-10].

The functional properties of articular cartilage are dependent on this unique structure and biochemical composition [11-13]. Confined and unconfined compression tests are commonly used to determine the material properties of articular cartilage. When cartilage is loaded in compression, a loss of tissue volume occurs due to fluid exudation from the tissue. These effects give rise to time-dependent viscoelastic behaviours such as creep and stress relaxation [2]. During stress relaxation testing, upon reaching equilibrium no hydraulic fluid

pressurization exists within the tissue and the intrinsic elastic properties of the solid matrix can be determined [14]. Previous studies have revealed that the compressive modulus increases with depth from the articular surface which correlates to an increase in sulphated glycosaminoglycan (sGAG) content [12, 15-19]. A certain amount of strain softening has also been observed during compressive loading [20, 21] which can be attributed, at least in part, to unloading of the vertically aligned collagen fibres that are initially pre-stressed due to tissue swelling [22]. The tensile strength and stiffness of the tissue is mainly attributed to both the amount and organisation of the collagen fibres and is highest in the superficial tangential zone [23, 24]. Hydraulic permeability, inversely correlated to collagen content and fixed charge density [16], is lowest in the superficial tangential zone. This is speculated to be due to the zone's high collagen content, the collagen fibres' tightly packed organisation and their tangential orientation to the articular surface [14, 25, 26].

While the relationship between the depth dependent composition of articular cartilage and its equilibrium mechanical properties have been well established, less is known about the depth dependent dynamic properties of the tissue and how they depend on the tissue's composition and structural organisation. During dynamic loading the apparent stiffness of the tissue is dependent on fluid pressurisation, which in turn is a function of the hydraulic permeability of the solid matrix. Such fluid pressurisation has been shown to initially support over 90% of the load applied to articular cartilage [27]. While the collagen network plays a key role in determining the permeability of articular cartilage, it further contributes to the tissue's ability to generate fluid load support by limiting radial expansion during compressive loading [11, 28]. Together these findings would suggest that the superficial region of the tissue, where the collagen network is a tightly packed and highly organised structure, would play a key role in determining the dynamic properties of the tissue. While the compressive modulus of this superficial region is lower than the rest of the tissue [29-32], it has been

demonstrated that upon removal of this layer the tissue is more susceptible to damage from impact loading [33]. The hypothesis of this study is that removal of the superficial region will influence both the flow dependent and independent properties of articular cartilage, leading to a reduction in the dynamic modulus of the remaining tissue. Elucidating the role of this region of the tissue in determining the functional properties of articular cartilage is critically important given that disruption to the superficial zone is often associated with the initiation and/or progression of osteoarthritis.

2. Materials and methods

2.1. Sample preparation

24 osteochondral cores were harvested from the medial and lateral trochlear ridges of the femoropatellar groove of three 4-month-old porcine knee joints within 3h of sacrifice; specimens were pooled from three different animals. Of these 24 cores, 16 were selected for mechanical testing. Cores (6mm diameter) were isolated normal to the articular surface using the Osteochondral Autograft Transfer System (Athrex, Naples, FL, USA) to a maximum depth of 20mm. After coring the subchondral bone was trimmed to approximately 2mm using a custom made cutting tool. The specimens were stored in phosphate buffered saline (PBS) solution (0.15M) and frozen at -80°C until the day of use. On each day of mechanical testing an individual core was thawed to room temperature by immersion in PBS solution and the height of the articular cartilage and respective subchondral bone was measured microscopically (Mitutoyo UK Ltd., Andover, UK) at four sites around the perimeter of the core, the cartilage-bone interface identified and marked using permanent ink. Osteochondral cores were first tested in confined or unconfined compression, and then cut into sections for layer specific testing.

2.2. Mechanical Testing-Full Thickness Osteochondral Cores

Osteochondral cores (n=9) were transferred to a confined compression chamber (Fig. 1A) and attached to a standard materials testing machine with a 20N pancake load cell (Zwick Roell Z005, Germany; resolution <0.5%). A preload of 0.05N was applied to ensure contact between the articular surface and the porous indenter (30μm porosity, Aegis Advanced Materials Ltd., Worcestershire, UK). Cores were kept hydrated through immersion in a PBS bath at room temperature. Stress relaxation testing was performed, where a series of compressive strains were applied in increasing steps of 10% strain to a maximum of 30% strain. At each strain increment, peak strain was achieved within 500 seconds and the equilibrium stress was recorded after a relaxation period of 1800 seconds (Fig. 1B). Preliminary tests revealed that 1800 seconds was a sufficient relaxation period to allow the samples to fully equilibrate at all loading magnitudes previously outlined. A 1% amplitude sinusoidal strain was superimposed directly after relaxation at each static strain increment at a frequency of 1Hz for five cycles at a 0.01%/s strain rate (Fig. 1B). The aggregate modulus was calculated as the equilibrium force divided by the specimen's cross sectional area divided by the applied strain, whilst the dynamic modulus was calculated as the average force amplitude divided by the specimens cross sectional area divided by the average strain amplitude for all cycles. After dynamic testing the superficial region of the cartilage was removed (Fig. 1C) using customised cutting tools for further testing in confined and unconfined compression. To ensure removal of the entire superficial region, and upon review of histological characterisation (Figs. 2 and 4), this section was taken as the top 25% of the total cartilage thickness from the articular surface [17, 34-36]. The remaining osteochondral core was then placed back into the confined compression chamber and retested using the same test sequence as outlined above.

For unconfined compression testing (Fig. 1D), osteochondral cores (n=7) were placed between two impermeable steel platens with and without their respective superficial regions. An identical testing regime to that described for confined testing was implemented, consisting of both stress relaxation and dynamic compression testing.

2.3. Layer Specific Testing

In order to elucidate the layer specific material properties individual layers were tested without the subchondral bone in confined and unconfined compression under the same testing sequence as was applied to the osteochondral cores. The superficial region, mean thickness of 0.9368 (0.71, 1.1637) mm, was taken as the cartilage section previously removed and the remainder of the articular cartilage after removal of the subchondral bone and calcified cartilage measured a mean thickness of 2.222 (2.1023, 2.3420) mm. Experimental data in the form of force/time stress relaxation curves were fit to a linear bi-phasic model for a known strain and aggregate modulus (H_A) in order to determine the layer specific average permeability of the different articular cartilage regions in confined compression. To evaluate the stress strain response, the axial normal stress can be evaluated at the interface with the porous indenter during the relaxation phase ($t \geq t_0$) by:

$$\frac{\sigma_a(t)}{H_A} = -P_e^w \left\{ \frac{t_0}{\tau} + \frac{2}{\pi^2} \sum_{n=1}^{\infty} e^{-n^2\pi^2\frac{t}{\tau}} \left(e^{n^2\pi^2\frac{t_0}{\tau}} - 1 \right) \right\} \text{ , where } P_e^w = \frac{V_0 h}{H_A k} \text{ and } \tau = \frac{h^2}{H_A k}$$

Here, V_0 is the loading velocity and h is the specimen thickness. Optimised values of *k* were determined by minimising the difference between predicted and experimental stress time profiles $\sigma_a(t)$ using a least squares method [17].

2.4. Biochemical Analysis

The wet mass of all mechanically tested layer specific slices was recorded and the samples were frozen for subsequent biochemical analysis. Samples were digested in papain (125

lg/mL) in 0.1 M sodium acetate, 5 mM cysteine HCl, 0.05 M EDTA, pH 6.0 (all from Sigma-Aldrich, Dublin, Ireland) at 60 °C under constant rotation for 18h. Aliquots of the digested samples were assayed separately for collagen and sulphated GAG content. The proteoglycan content was estimated by quantifying the amount of sulfated GAG using the dimethylmethylene blue dye-binding assay (Blyscan, Biocolor Ltd., Northern Ireland), with a chondroitin sulfate standard. Total collagen content was determined by measuring the hydroxyproline content using a hydroxyproline-to-collagen ratio of 1:7.69 [37]. Each biochemical constituent (hydroxyproline and GAG) was normalized to the tissue wet weight.

2.5. Histological Analysis

Osteochondral cores were fixed in 4% paraformaldehyde overnight at 4°C. Tissues were decalcified in 5% formic acid, 95% DI H_2O and secured on a gyro rocker at 40revs/min for approximately 30 days. Samples were checked each week and returned to fresh solution if not deemed completely decalcified. Once each sample appeared fully decalcified they were sliced in half along the vertical axis, dehydrated, wax embedded and sectioned at 8μm. Sections were stained with safranin O for sGAG and picrosirius red for collagen and subsequently imaged on an Olympus Bx41 microscope equipped with a 30-bit CCD camera (Mason Technology, Dublin, Ireland).

In order to quantitatively analyse these histologically stained sections, TIFF images were converted to greyscale and stored as 8 bits per sampled pixel which allows 256 intensity levels or shades of grey. Among these light intensity levels, black or complete lack of light is represented numerically as zero whilst pure white is represented as 255. Converted images were analysed for intensity levels with depth from the articular surface using MATLAB 7.0. (Mathworks, Cambridge, UK).

2.6 Polarised Light Microscopy (PLM)

Polarised light microscopy is an optical microscopy technique used to study structural orientation of anisotropic materials such as articular cartilage. Essentially, a polariser filter placed after the light source on a microscope ensures only linearly polarised light is transmitted to the specimen. Optically anisotropic materials change the direction of the polarised light, which is known as birefringence [38]. PLM exploits the natural birefringence of cartilage which varies through the depth of the tissue due to the orientation and the alignment of collagen fibres. As this birefringence can be fairly weak and difficult to detect, picrosirius red staining was performed to enhance visualisation with polarised light [39]. In an effort to reduce birefringence of the surrounding matrix all GAGs were digested prior to imaging. Briefly, sections were incubated for 90 min at 37°C in a 0.5% pre-warmed papain solution (pH 4.43) and then rinsed in distilled water prior to staining [40]. In articular cartilage, PLM reveals the highly organised collagen structure of the superficial region and deep zone as two birefringent regions, separated by a non-birefringent and hence randomly organised middle zone [38].

2.7. Statistical Analysis

Statistical analysis was performed using a two way ANOVA with Tukey's post-hoc test for multiple comparisons, whilst two sample t-tests were used for unpaired data sets. All tests were performed using the statistical software package MINITAB 15.1 (Minitab Ltd., Coventry, UK). Numerical and graphical results are displayed as mean with uncertainty expressed by 95% confidence intervals (CIs): mean (upper limit, lower limit). Significance was accepted at $p \leq 0.05$ or as indicated. Sample numbers varied according to respective comparison and are outlined in the results section of this manuscript.

3. Results

Polarised light microscopy revealed intensely birefringent and hence highly organised collagen structures in the superficial region and deep zone of the tissue; fibrils appear orientated parallel to the articular surface in the superficial region and perpendicular to the subchondral bone in the deep zone (Fig. 2).

Biochemical analysis revealed a lower ($p=0.027$) sGAG content in the superficial region compared to the remaining tissue, with no significant difference ($p=0.426$) in the total collagen content between the two regions (Fig. 3). Histological analysis with safranin O staining correlated with the results of the sGAG biochemical assay, displaying decreased staining in the superficial region. The picrosirius red stained sections demonstrated a more complex spatial distribution of collagen through the depth of the tissue, with the superficial and deep regions staining intensely for collagen and a more moderate staining in the middle region (Fig. 2). Significantly higher light intensities were measured in the superficial region of the safranin O stained sections ($p=0.026$) (Fig. 4), indicating less intense staining in this region of the tissue and hence a lower sGAG content. Picrosirius red stained sections displayed highest light intensity in the middle zone, with lower intensity values in the superficial and deep regions suggesting higher collagen content in these zones (Fig. 4). Hence, removal of the superficial region exposed a low-collagen region. This observation could not have been made from bulk biochemical analysis alone.

Cartilage thickness averaged 3.051 (2.516, 3.586) mm for full thickness osteochondral cores and 2.435 (1.92, 2.95) mm after removal of the superficial region; approximately 25 (19.01, 31.95) % of the total cartilage thickness. The aggregate moduli determined from confined compression testing of osteochondral cores (Fig. 5A) significantly increased ($p=0.0035$) at 10% strain after removal of the superficial region by 50.4% (from 0.76 (0.65, 0.88) MPa to 1.1 (0.88, 1.3) MPa). The compressive stiffness in unconfined

compression (Fig.5B) also significantly increased ($p=0.0365$) by 26.6% (from 0.75 (0.66, 0.84) MPa to 0.93 (0.86, 1.01) MPa). In contrast, the confined dynamic modulus significantly decreased at each strain level of 10, 20 and 30% ($p=0.0053$, $p<0.0001$ and $p=0.0049$ respectively) upon removal of the superficial region by 24% (from 29.45 (26.64, 32.25) MPa to 22.26 (19.97, 24.54) MPa), 33.3% (from 43.75 (40.44, 47.07) MPa to 29.07 (25.91, 32.22) MPa) and 25.4% (from 42.09 (31.43, 52.76) MPa to 30.59 (26.6, 34.58) MPa) respectively. The ratio of the peak stress to equilibrium stress during stress relaxation testing (Fig. 6) at 10% strain in unconfined compression significantly reduced ($p=0.006$) upon removal of the superficial region from 2.07 (1.89, 2.25) to 1.68 (1.47, 1.9) suggesting a reduced ability to maintain fluid load support.

Layer specific mechanical testing revealed a similar trend of increasing aggregate and equilibrium moduli with depth, whilst in general the confined and unconfined dynamic moduli of the superficial region was lower than the remaining cartilage (Fig. 7A, B).

Experimental data fit to a linear bi-phasic model of articular cartilage in confined compression revealed a significantly lower hydraulic permeability in the superficial region (1.98×10^{-15} (1.03×10^{-15}, 2.93×10^{-15}) $m^4/N{\cdot}s$) compared to the remaining cartilage (3.22×10^{-15} (2.46×10^{-15}, 3.97×10^{-15}) $m^4/N{\cdot}s$) when tested in isolation ($p=0.028$).

4. Discussion

The objective of this study was to test the hypothesis that removal of the superficial region of the tissue will influence both the flow dependent and independent properties of articular cartilage, leading to an increase in the equilibrium modulus but a reduction in the dynamic modulus of the tissue. In confined compression, significant increases in the aggregate modulus (H_A) of the osteochondral cores upon removal of the superficial region were observed, which is in agreement with the literature [12, 14, 18, 28, 41]. This rise in stiffness

corresponded with a significant increase in sGAG content with depth from the articular surface [42-45]. However, while removal of the superficial region increased the aggregate modulus of the remaining tissue, a significant reduction in the dynamic modulus was observed. This is despite the fact that when tested in isolation the dynamic modulus of this layer at high offset strains was significantly lower than the remaining tissue in both confined and unconfined compression as has been observed in previous studies [33, 46], confirming that in isolation the superficial region is the softest part of the tissue in compression.

While the finding of an increased equilibrium modulus upon removal of the superficial region is intuitive, the finding that the dynamic modulus decreased with removal of this soft layer requires further discussion. The reduction in dynamic modulus may be partially explained by geometric effects. Consider first the gel diffusion time, given by $\tau_m = {\delta^2}/{H_A k}$ (*s*), where δ in confined compression is given by the height (m) of the sample, $H_A(Pa)$ is the aggregate modulus and (^{4} $^{-1}$ $^{-1}$) is the hydraulic permeability [17, 47]. By reducing the sample height, this effectively reduces the gel diffusion time. Therefore for any given loading frequency, this would imply lower interstitial fluid pressurisation based on the assumptions of a linear biphasic model of articular cartilage [17, 48]. This reduction in fluid pressurisation could contribute to the lower dynamic modulus observed upon removal of the superficial region. The reduced sample height may also partially explain the lower dynamic modulus values of the isolated regions in confined compression versus the full thickness osteochondral cores.

Another explanation for this reduction in dynamic modulus is the significantly lower ($p=0.028$) permeability in the superficial region compared to the remaining cartilage (obtained from fits of our data to a linear biphasic model). This low permeability region essentially acts as a barrier to fluid flow and its removal is speculated to lead to reduced fluid pressurisation in the tissue during dynamic loading. It has previously been hypothesised that

304 the permeability of this region of the tissue is due to the high concentration of tightly woven
305 collagen fibrils orientated parallel to the articular surface resulting in a system of much
306 narrower channels offering a greater resistance to fluid flow [1, 14, 26, 49]. Once compressed
307 this fibrillar sheet is compacted and further restricts fluid exudation [50]. After removal of the
308 superficial region, more fluid can escape during cyclic loading than in intact tissues.
309 Histological analysis of the tissues tested as part of this study (Fig. 2) confirmed a high
310 collagen content in the superficial region, with PLM analysis revealing closely packed
311 collagen fibrils orientated parallel to the articular surface [51]. It has previously been found
312 that with removal of the upper most 100 microns of tissue, equilibrium deformation is
313 reached sooner compared to the intact articular cartilage specimen and furthermore removal
314 of the top surface caused a substantial increase in the quantity of fluid exchanged during each
315 loading cycle, also suggesting an increase in the permeability of the tissue [32] and
316 supporting our observations.

317 Overall, the present results indicate that removal of the superficial region leads to a
318 deterioration in the transient, i.e. fluid mediated, load bearing properties of cartilage tissue via
319 both geometric and permeability effects. Decoupling these geometric and permeability effects
320 further requires additional work.

321 During unconfined compression fluid will exude radially out of the sides of the
322 cylindrical samples. As all sample diameters were identical geometric effects will play no
323 role. It should be noted that with this testing modality the tissue is allowed to bulge radially
324 and collagen fibres, particularly those orientated perpendicular to the direction of loading in
325 the superficial region, can play a key role in maintaining fluid load support by preventing
326 lateral expansion of the tissue [11, 28, 52-54]. This may explain the significant drop
327 ($p=0.006$) in the ratio of peak stress to equilibrium stress at 10% strain observed during
328 unconfined compression upon removal of the superficial region of the tissue (Fig. 6).

A significant increase in dynamic stiffness with increasing magnitudes of the offset compressive strain was observed in confined and unconfined compression for osteochondral tissue cores and isolated layers (Figs. 5, 7). This strain dependent increase may be due to a deformation induced decrease in tissue permeability, i.e. increasing compaction of the collagen network offering increased frictional resistance to the flow of interstitial fluid [21, 55-57]. In a similar manner, compressive strain of the cartilage will cause compaction of the proteoglycans in the tissue which will in turn increase the fixed charge density in the tissue further decreasing tissue permeability [25, 26].

There are potential limitations associated with this study. The porcine tissue tested was not skeletally mature and therefore its collagen architecture does not equate that of fully mature samples, although our analysis confirmed a tissue organisation that mimics key aspects of the architecture of adult cartilage (Fig. 2C). Slicing the cartilage into layers may have an impact on the functional properties of the tissue by disturbing the intrinsic continuum structure [30] and possibly damaging the tissue. Although scanning electron microscopy has previously demonstrated that the surface of both cut and intact articular cartilage display similar collagen fibril architecture [31], artefacts due to cutting cannot be ruled out and the isolation of specific zones may have compound effects on their functional properties. In an effort to ensure full removal of the superficial region the top 25 (19.01, 31.95) % of the total cartilage thickness was cut from the articular surface. Whilst a larger proportion than what is classically defined as the superficial zone, this percentage ratio was based on previous studies [17, 35-37] and our own analysis of picrosirius red stained histological sections (Fig.2) and pixel intensity profiles (Fig.4) which show a dense collagen content in the upper ~25% of the total cartilage thickness. In tissue that has reached full skeletal maturity, the superficial zone of the tissue is thinner, pointing to the dynamic nature of collagen modelling and remodelling during skeletal development [58]. Preliminary studies whereby only the top 10% of the total

cartilage thickness was removed (data not shown) showed no statistically significant decrease in the dynamic modulus of the remaining tissue upon its removal. This suggested that the entire superficial region with its high collagen content was not removed, although geometrical effects as discussed above may also play a role. Another possible limitation to the experimental approach adopted in this study is that part of the transitional zone of the tissue may also have been removed during slicing. The biomechanical function of the transitional zone has yet to be fully elucidated. Therefore as it isn't possible to accurately separate the superficial region from the transitional zone using the present experimental setup, we cannot exclude the possibility that removal of part of this region of the tissue is also contributing to our experimental findings.

A biomechanical failure of the collagen network in the superficial tangential zone is postulated in many hypotheses as related to the development of osteoarthritis [14, 59, 60] Computational models have also been used to demonstrate how a viable superficial zone is critical to achieving long term survival in repairing articular cartilage [61, 62]. This study demonstrates that although this layer is less stiff than the remainder of the tissue in compression, it plays a key role in elevating the dynamic material properties of the tissue. This is presumably achieved by generating higher fluid load support due to its dense collagen fibre network and organisation and hence low permeability. Taken together these studies highlight the importance of understanding the role of the superficial region in articular cartilage development and degeneration, and in the design of novel tissue engineering approaches to cartilage regeneration. Future studies will explore how and why these structural, compositional and functional changes emerge in articular cartilage with skeletal maturity and what role the local environment within the developing joint plays in driving these changes.

Conflict of interest

The author declares that there is no conflict of interest.

Acknowledgements

This study was funded by the Science Foundation Ireland (SFI) under the President of Ireland Young Researcher Award (PIYRA) 08/YI5/B1336 and IRCSET (G30345).

Author Contribution

All authors contributed equally to the conception and design of this study. Acquisition and analysis of data and article drafting was carried out by A.G. All authors approved the final draft of the manuscript.

References

1. Freeman, M.A.R., Adult Articular Cartilage. 1973, Great Britain: Sir Issac Pitman and Sons LTD.
2. Mow, V.C. and X.E. Guo, Mechano-electrochemical properties of articular cartilage: Their inhomogeneities and anisotropies, in Annual Review of Biomedical Engineering. 2002. p. 175-209.
3. Stockwell, R.A. Changes in the acid glycosaminoglycan content of the matrix of ageing human articular cartilage. Annals of the Rheumatic Diseases 1970; 29(5):509-515.
4. Guilak, F., A. Ratcliffe, and V.C. Mow. Chondrocyte deformation and local tissue strain in articular cartilage: A confocal microscopy study. Journal of Orthopaedic Research 1995; 13(3):410-421.
5. Ge, Z., C. Li, B.C. Heng, G. Cao, and Z. Yang. Functional biomaterials for cartilage regeneration. Journal of Biomedical Materials Research - Part B 2012; 00B:000-000.
6. Armstrong, C.G. and V.C. Mow. Variations in the intrinsic mechanical properties of human articular cartilage with age, degeneration, and water content. Journal of Bone and Joint Surgery - Series A 1982; 64(1):88-94.
7. Benninghoff, A. Form und Bau der Gelenkknorpel in ihren Beziehungen zur Funktion - Zweiter Teil: Der Aufbau des Gelenkknorpels in seinen Beziehungen zur Funktion. Zeitschrift fur Zellforschung und Mikroskopische Anatomie 1925; 2(5):783-862.
8. Mow, V.C. and R. Huiskes, Basic Orthopaedic Biomechanics and Mechano-Biology. 3rd ed. 2005, Philadelphia: Lippincott Williams & Wilkins.
9. Redler, I., V.C. Mow, M.L. Zimny, and J. Mansell. The ultrastructure and biomechanical significance of the tidemark of articular cartilage. Clinical Orthopaedics and Related Research 1975; no.112:357-362.

10. van Turnhout, M.C., S. Kranenbarg, and J.L. van Leeuwen. Contribution of postnatal collagen reorientation to depth-dependent mechanical properties of articular cartilage. Biomechanics and Modeling in Mechanobiology 2010:1-11.
11. Ateshian, G.A. The role of interstitial fluid pressurization in articular cartilage lubrication. Journal of Biomechanics 2009; 42(9):1163-1176.
12. Julkunen, P., T. Harjula, J. Iivarinen, J. Marjanen, K. Seppanen, T. Narhi, J. Arokoski, M.J. Lammi, P.A. Brama, J.S. Jurvelin, and H.J. Helminen. Biomechanical, biochemical and structural correlations in immature and mature rabbit articular cartilage. Osteoarthritis and Cartilage 2009; 17(12):1628-1638.
13. Wilson, W., J.M. Huyghe, and C.C. Van Donkelaar. Depth-dependent compressive equilibrium properties of articular cartilage explained by its composition. Biomechanics and Modeling in Mechanobiology 2007; 6(1-2):43-53.
14. Setton, L.A., W. Zhu, and V.C. Mow. The biphasic poroviscoelastic behavior of articular cartilage: Role of the surface zone in governing the compressive behavior. Journal of Biomechanics 1993; 26(4-5):581-592.
15. Chen, S.S., Y.H. Falcovitz, R. Schneiderman, A. Maroudas, and R.L. Sah. Depth-dependent compressive properties of normal aged human femoral head articular cartilage: Relationship to fixed charge density. Osteoarthritis and Cartilage 2001b; 9(6):561-569.
16. Maroudas, A. Balance between swelling pressure and collagen tension in normal and degenerate cartilage. Nature 1976b; 260(5554):808-809.
17. Mow, V.C., S.C. Kuei, W.M. Lai, and C.G. Armstrong. Biphasic creep and stress relaxation of articular cartilage in compression: Theory and experiments. Journal of Biomechanical Engineering 1980; 102(1):73-84.
18. Schinagl, R.M., D. Gurskis, A.C. Chen, and R.L. Sah. Depth-dependent confined compression modulus of full-thickness bovine articular cartilage. Journal of Orthopaedic Research 1997; 15(4):499-506.
19. Wang, C.C., J.M. Deng, G.A. Ateshian, and C.T. Hung. An automated approach for direct measurement of two-dimensional strain distributions within articular cartilage under unconfined compression. J Biomech Eng 2002; 124(5):557-67.
20. Ateshian, G.A., V. Rajan, N.O. Chahine, C.E. Canal, and C.T. Hung. Modeling the matrix of articular cartilage using a continuous fiber angular distribution predicts many observed phenomena. Journal of Biomechanical Engineering 2009; 131(6).
21. Chahine, N.O., C.C.B. Wang, C.T. Hung, and G.A. Ateshian. Anisotropic strain-dependent material properties of bovine articular cartilage in the transitional range from tension to compression. Journal of Biomechanics 2004; 37(8):1251-1261.
22. Nagel, T. and D.J. Kelly. The influence of fiber orientation on the equilibrium properties of neutral and charged biphasic tissues. Journal of Biomechanical Engineering 2010; 132(11):114506.
23. Roth, V. and V.C. Mow. The intrinsic tensile behavior of the matrix of bovine articular cartilage and its variation with age. Journal of Bone and Joint Surgery - Series A 1980; 62(7):1102-1117.
24. Williamson, A.K., A.C. Chen, K. Masuda, E.J.M.A. Thonar, and R.L. Sah. Tensile mechanical properties of bovine articular cartilage: Variations with growth and relationships to collagen network components. Journal of Orthopaedic Research 2003; 21(5):872-880.
25. Mansour, J.M. and V.C. Mow. The permeability of Articular Cartilage under Compressive Strain and at High Pressures. Journal of Bone and Joint Surgery 1976; 58-A(4):509-516.

26. Maroudas, A. and P. Bullough. Permeability of articular cartilage. Nature 1968; 219(5160):1260-1261.
27. Soltz, M.A. and G.A. Ateshian. Interstitial Fluid Pressurization during Confined Compression Cyclical Loading of Articular Cartilage. Annals of Biomedical Engineering 2000; 28(2):150-159.
28. Kiviranta, P., J. Rieppo, R.K. Korhonen, P. Julkunen, J. Toyras, and J.S. Jurvelin. Collagen network primarily controls poisson's ratio of bovine articular cartilage in compression. Journal of Orthopaedic Research 2006; 24(4):690-699.
29. Bevill, S.L., A. Thambyah, and N.D. Broom. New insights into the role of the superficial tangential zone in influencing the microstructural response of articular cartilage to compression. Osteoarthritis and Cartilage 2010; 18(10):1310-1318.
30. Glaser, C. and R. Putz. Functional anatomy of articular cartilage under compressive loading quantitative aspects of global, local and zonal reactions of the collagenous network with respect to the surface integrity. Osteoarthritis and Cartilage 2002; 10(2):83-99.
31. Torzilli, P.A. Effects of temperature, concentration and articular surface removal on transient solute diffusion in articular cartilage. Medical and Biological Engineering and Computing 1993; 31(4 SUPPL.):S93-S98.
32. Torzilli, P.A., D.A. Dethmers, D.E. Rose, and H.F. Schryuer. Movement of interstitial water through loaded articular cartilage. Journal of Biomechanics 1983; 16(3):169-179.
33. Rolauffs, B., C. Muehleman, J. Li, B. Kurz, K.E. Kuettner, E. Frank, and A.J. Grodzinsky. Vulnerability of the superficial zone of immature articular cartilage to compressive injury. Arthritis & Rheumatism 2010; 62(10):3016-3027.
34. Canal, C.E., C.T. Hung, and G.A. Ateshian. Two-dimensional strain fields on the cross-section of the bovine humeral head under contact loading. Journal of Biomechanics 2008; 41(15):3145-3151.
35. Rieppo, J., E. Halmesmaki, U. Sittonen, M.S. Laasanen, J. Toyras, I. Kiviranta, M.M. Hyttinen, J.S. Jurvelin, and H.J. Helminen. Histological Differences of Human, Bovine, and Porcine Cartilage. in 49th Annual Meeting of the Orthopaedic Research Society (poster). 2003. New Orleans, Louisiana.
36. Xia, Y. Averaged and Depth-Dependent Anisotropy of Articular Cartilage by Microscopic Imaging. Seminars in Arthritis and Rheumatism 2008; 37(5):317-327.
37. Ignat'eva, N.Y., N.A. Danilov, S.V. Averkiev, M.V. Obrezkova, V.V. Lunin, and E.N. Sobol. Determination of hydroxyproline in tissues and the evaluation of the collagen content of the tissues. Journal of Analytical Chemistry 2007; 62(1):51-57.
38. Changoor, A., N. Tran-Khanh, S. Méthot, M. Garon, M.B. Hurtig, M.S. Shive, and M.D. Buschmann. A polarized light microscopy method for accurate and reliable grading of collagen organization in cartilage repair. Osteoarthritis and Cartilage 2011; 19(1):126-135.
39. Király, K., M.M. Hyttinen, T. Lapveteláinen, M. Elo, I. Kiviranta, J. Dobai, L. Módis, H.J. Helminen, and J.P.A. Arokoski. Specimen preparation and quantification of collagen birefringence in unstained sections of articular cartilage using image analysis and polarizing light microscopy. Histochemical Journal 1997; 29(4):317-327.
40. Lecocq, M., C.A. Girard, U. Fogarty, G. Beauchamp, H. Richard, and S. Laverty. Cartilage matrix changes in the developing epiphysis: Early events on the pathway to equine osteochondrosis? Equine Veterinary Journal 2008; 40(5):442-454.
41. Laasanen, M.S., J. Toyras, R.K. Korhonen, J. Rieppo, S. Saarakkala, M.T. Nieminen, J. Hirvonen, and J.S. Jurvelin. Biomechanical properties of knee articular cartilage. Biorheology 2002; 40(1-3):133-140.

42. Canal Guterl, C., C.T. Hung, and G.A. Ateshian. Electrostatic and non-electrostatic contributions of proteoglycans to the compressive equilibrium modulus of bovine articular cartilage. Journal of Biomechanics 2010; 43(7):1343-1350.
43. Lu, X.L. and V.C. Mow. Biomechanics of articular cartilage and determination of material properties. Medicine and Science in Sports and Exercise 2008; 40(2):193-199.
44. Poole, C.A., M.H. Flint, and B.W. Beaumont. Chondrons in cartilage: Ultrastructural analysis of the pericellular microenvironment in adult human articular cartilages. Journal of Orthopaedic Research 1987; 5(4):509-522.
45. Williamson, A.K., A.C. Chen, and R.L. Sah. Compressive properties and function-composition relationships of developing bovine articular cartilage. Journal of Orthopaedic Research 2001; 19(6):1113-1121.
46. Treppo, S., H. Koepp, E.C. Quan, A.A. Cole, K.E. Kuettner, and A.J. Grodzinsky. Comparison of biomechanical and biochemical properties of cartilage from human knee and ankle pairs. Journal of Orthopaedic Research 2000; 18(5):739-748.
47. Morel, V. and T.M. Quinn. Cartilage injury by ramp compression near the gel diffusion rate. Journal of Orthopaedic Research 2004; 22(1):145-151.
48. Suh, J.K., Z. Li, and S.L.Y. Woo. Dynamic behavior of a biphasic cartilage model under cyclic compressive loading. Journal of Biomechanics 1995; 28(4):357-364.
49. Maroudas, A. and C. Bannon. Measurement of swelling pressure in cartilage and comparison with osmotic pressure of constituent proteoglycans. Biorheology 1981; 18(3-6):619-632.
50. Torzilli, P.A. Mechanical response of articular cartilage to an oscillating load. Mechanics Research Communications 1984; 11(1):75-82.
51. Rieppo, J., J. Hallikainen, J.S. Jurvelin, I. Kiviranta, H.J. Helminen, and M.M. Hyttinen. Practical considerations in the use of polarized light microscopy in the analysis of the collagen network in articular cartilage. Microscopy Research and Technique 2008; 71(4):279-287.
52. Jurvelin, J.S., M.D. Buschmann, and E.B. Hunziker. Optical and mechanical determination of Poisson's ratio of adult bovine humeral articular cartilage. Journal of Biomechanics 1996; 30(3):235-241.
53. Korhonen, R.K., M.S. Laasanen, J. Toyras, J. Rieppo, J. Hirvonen, H.J. Helminen, and J.S. Jurvelin. Comparison of the equilibrium response of articular cartilage in unconfined compression, confined compression and indentation. Journal of Biomechanics 2002; 35(7):903-909.
54. Park, S., R. Krishnan, S.B. Nicoll, and G.A. Ateshian. Cartilage interstitial fluid load support in unconfined compression. Journal of Biomechanics 2003; 36(12):1785-1796.
55. Bursac, P.M., T.W. Obitz, S.R. Eisenberg, and D. Stamenovic. Confined and unconfined stress relaxation of cartilage: Appropriateness of a transversely isotropic analysis. Journal of Biomechanics 1999; 32(10):1125-1130.
56. Chen, A.C., W.C. Bae, R.M. Schinagl, and R.L. Sah. Depth- and strain-dependent mechanical and electromechanical properties of full-thickness bovine articular cartilage in confined compression. Journal of Biomechanics 2001a; 34(1):1-12.
57. Erne, O.K., J.B. Reid, L.W. Ehmke, M.B. Sommers, S.M. Madey, and M. Bottlang. Depth-dependent strain of patellofemoral articular cartilage in unconfined compression. Journal of Biomechanics 2005; 38(4):667-672.
58. Van Turnhout, M.C., H. Schipper, B. Engel, W. Buist, S. Kranenbarg, and J.L. Van Leeuwen. Postnatal development of collagen structure in ovine articular cartilage. BMC Developmental Biology 2010; 10.

59. Bank, R.A., M.T. Bayliss, F.P.J.G. Lafeber, A. Maroudas, and J.M. Tekoppele. Ageing and zonal variation in post-translational modification of collagen in normal human articular cartilage: The age-related increase in Non-Enzymatic Glycation affects biomechanical properties of cartilage. Biochemical Journal 1998; 330(1):345-351.
60. Buckwalter, J.A., H.J. Mankin, and A.J. Grodzinsky. Articular cartilage and osteoarthritis. Instructional course lectures 2005; 54:465-480.
61. Owen, J.R. and J.S. Wayne. Influence of a superficial tangential zone over repairing cartilage defects: Implications for tissue engineering. Biomechanics and Modeling in Mechanobiology 2006; 5(2-3):102-110.
62. Owen, J.R. and J.S. Wayne. Contact models of repaired articular surfaces: Influence of loading conditions and the superficial tangential zone. Biomechanics and Modeling in Mechanobiology 2010; 10(4):461-471.

List of Figures

Fig.1. Schematic representation of testing configurations. (A) Diagram illustrating confined compression; σ_a indicating axial stress is applied in the arrow direction, (B) loading protocol at increasing strain levels (10, 20 and 30 % strain). In addition, cyclic loading was applied at each strain level after equilibrium had been reached at 1% amplitude and 1Hz frequency (C) Graphic of an osteochondral core divided into layers: intact osteochondral core, less superficial region: remaining cartilage and subchondral bone, superficial region and remaining cartilage (D) diagram illustrating unconfined compression. During unconfined compression of the osteochondral cores radial displacement of the deepest cartilage layers are prevented by the attached subchondral bone.

Fig.2. Osteochondral sections stained with picrosirius red and safranin O from the femoral trochlear ridges. (A) Picrosirius red stained magnifications of a full thickness cartilage section, scale bar 200μm (Left). (B) Picrosirius red stained magnifications imaged using polarised light microscopy (PLM). A change in the direction of the polarised light known as birefringence occurs close to the articular surface and in the deep zone, allowing the visualisation of the differentiation between the highly organised superficial and deep zone and the non-birefringent middle zone; scale bar 50μm. (C) Safranin O stained magnifications displaying an increase in staining with depth correlating to an increase in sGAG content, scale bar 50μm.

Fig.3. (A) Sulphated glycosaminoglycan (sGAG) content and (B**)** total collagen content of superficial region and remaining cartilage disks of porcine articular cartilage per wet weight [%] obtained from the femoral trochlear ridges. Bars show the mean with 95% CI; n=6; donors=3. * $p = 0.027$.

Fig.4. Pixel intensity profiles of histological samples with depth from the articular surface of (A) safranin o stain and (B) picrosirius red stain. Figure (C) displays the average of these values correlating to specific regions; superficial region (SR) and the remaining cartilage. Bars show mean with 95% CI. The dashed line indicates the top 25% of the total cartilage thickness i.e. from the articular surface to the base of the cartilage. *p=0.026.

Fig.5. (A) Aggregate moduli and dynamic moduli in confined compression of full thickness osteochondral cores and less the superficial region of porcine articular cartilage obtained from the femoral trochlear ridges. Bars show the mean ± 95% CI, n=9. (B) Compressive stiffness ($\sigma_{equil}/\varepsilon$) and dynamic stiffness in unconfined compression of the same testing configuration as outlined above. Bars show the mean ± 95% CI, n=9. All dynamic testing was carried out at 1Hz freq. and 1% amplitude at increasing levels of offset strain ε: 10, 20 and 30%. Connecting line does not imply linear relationship with strain. In A and B, 'a' indicates a significant difference vs. 'Intact Osteochondral Core' (10% ε), 'b' indicates a significant difference vs. 'Intact Osteochondral Core' (20% ε), 'c' indicates a significant difference vs. 'Intact Osteochondral Core' (30% ε),'d' indicates a significant difference vs. 'Less Superficial Region' (10% ε). Specific *p* values for these differences are as follows: α:p=0.0035, β:p=0.0053, γ:p<0.0001, δ:p=0.0093, ε:p=0.0049, ζ:p=0.0015, η:p=0.0001, θ:p=0.0016, ι:p=0.0037, κ:p=0.0032, λ:p=0.0033.

Fig.6. Peak stress: equilibrium stress ratio in unconfined compression at increasing levels of offset strain ε: 10, 20 and 30% of full thickness osteochondral cores and less the superficial region of porcine articular cartilage obtained from the femoral trochlear ridges. Bars show the mean ± 95% CI, n=9. Connecting line does not imply linear relationship with strain.

Fig.7. (A) Aggregate moduli and dynamic moduli in confined compression of the superficial region and remaining cartilage disks of porcine articular cartilage obtained from the femoral trochlear ridges. Bars show the mean ± 95% CI, n=7. (B) Equilibrium moduli and dynamic

moduli in unconfined compression of the same testing configuration as outlined above. Bars show the mean ± 95% CI, n=7. All dynamic testing was carried out at 1Hz freq. and 1% amplitude at increasing levels of offset strain ε: 10, 20 and 30%. Connecting line does not imply linear relationship with strain. In A and B, 'a' indicates a significant difference vs. 'Superficial Region' (10% ε), 'b' indicates a significant difference vs. 'Superficial Region' (20% ε), 'c' indicates a significant difference vs. 'Superficial Region' (30% ε). Specific *p* values for these differences are as follows: α:p=0.05, β:p=0.0401, γ:p=0.0386, δ:p=0.0001, ε:p=0.0147, ζ:p=0.0185, η:p=0.0104.

Figure 1

Click here to download high resolution image

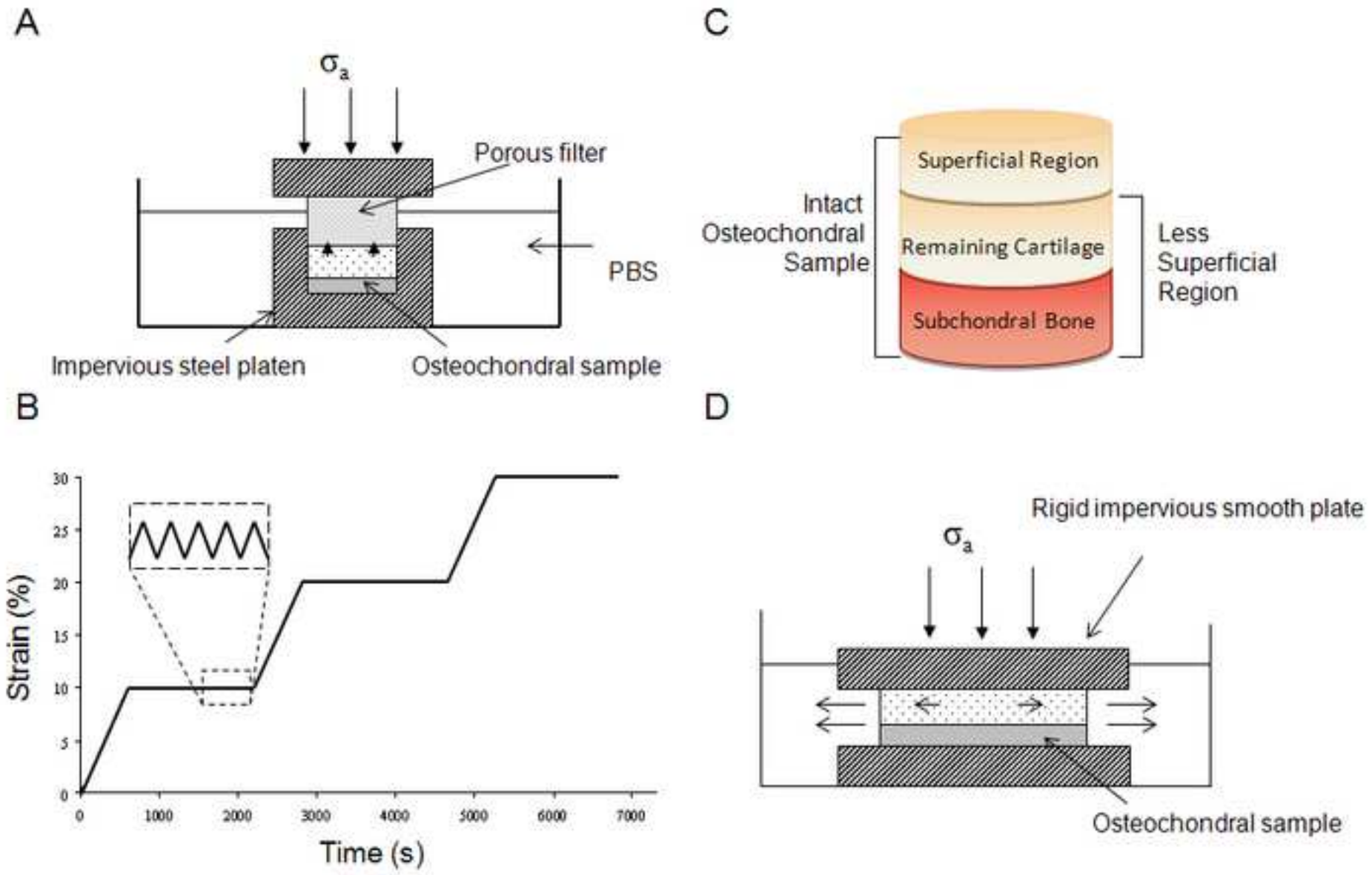

Figure 2

Click here to download high resolution image

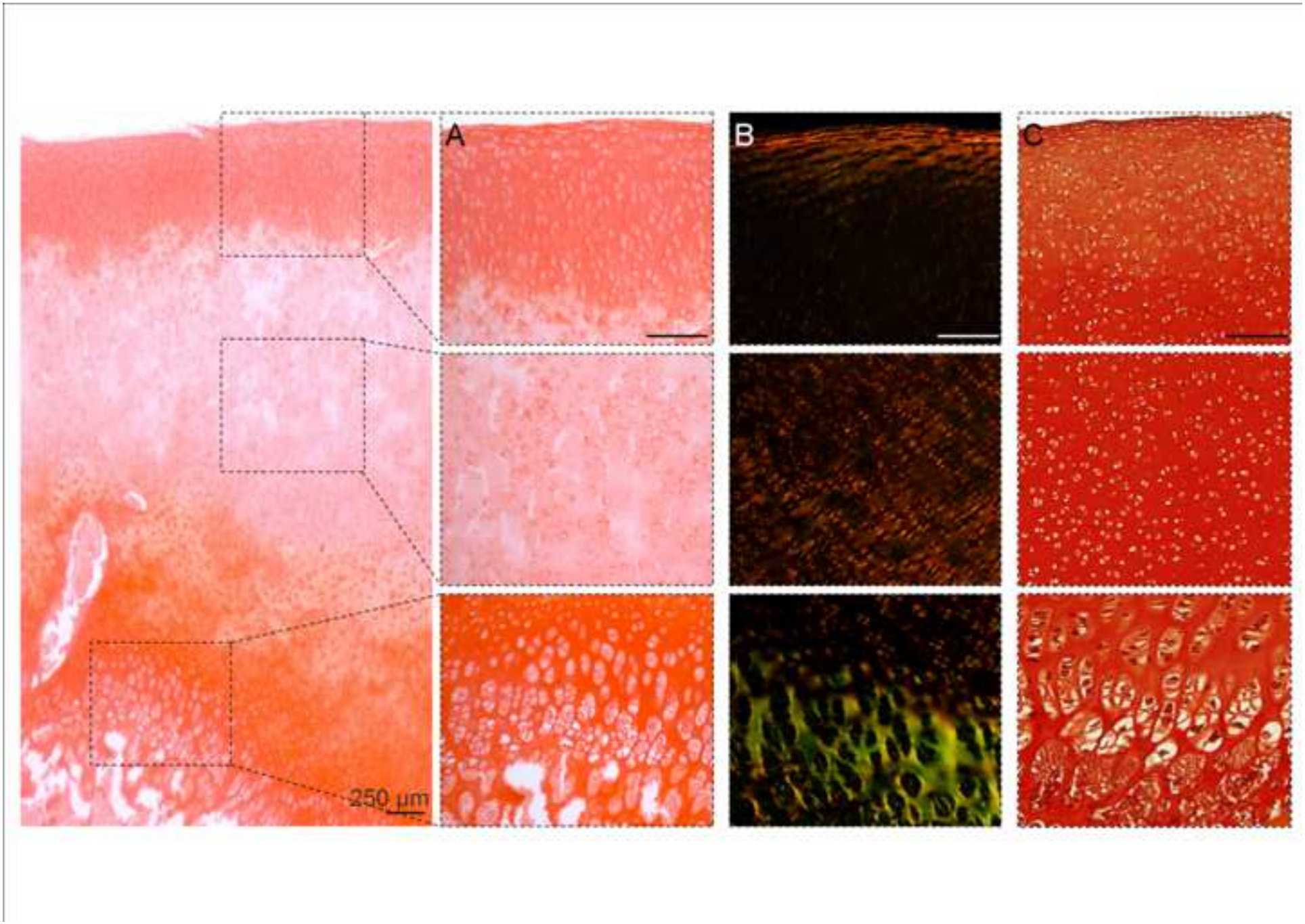

Figure 3

Click here to download high resolution image

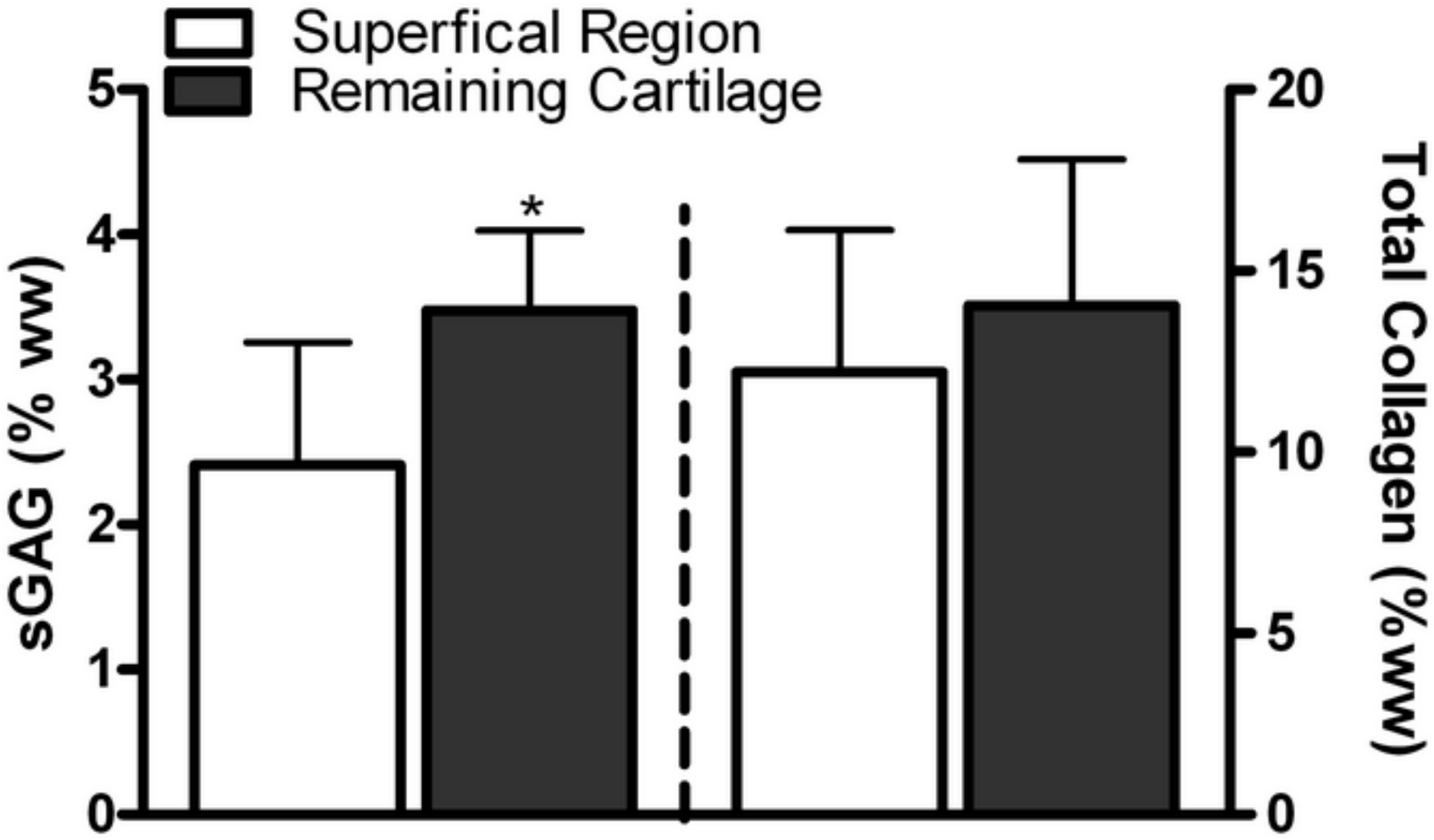

Figure 4

Click here to download high resolution image

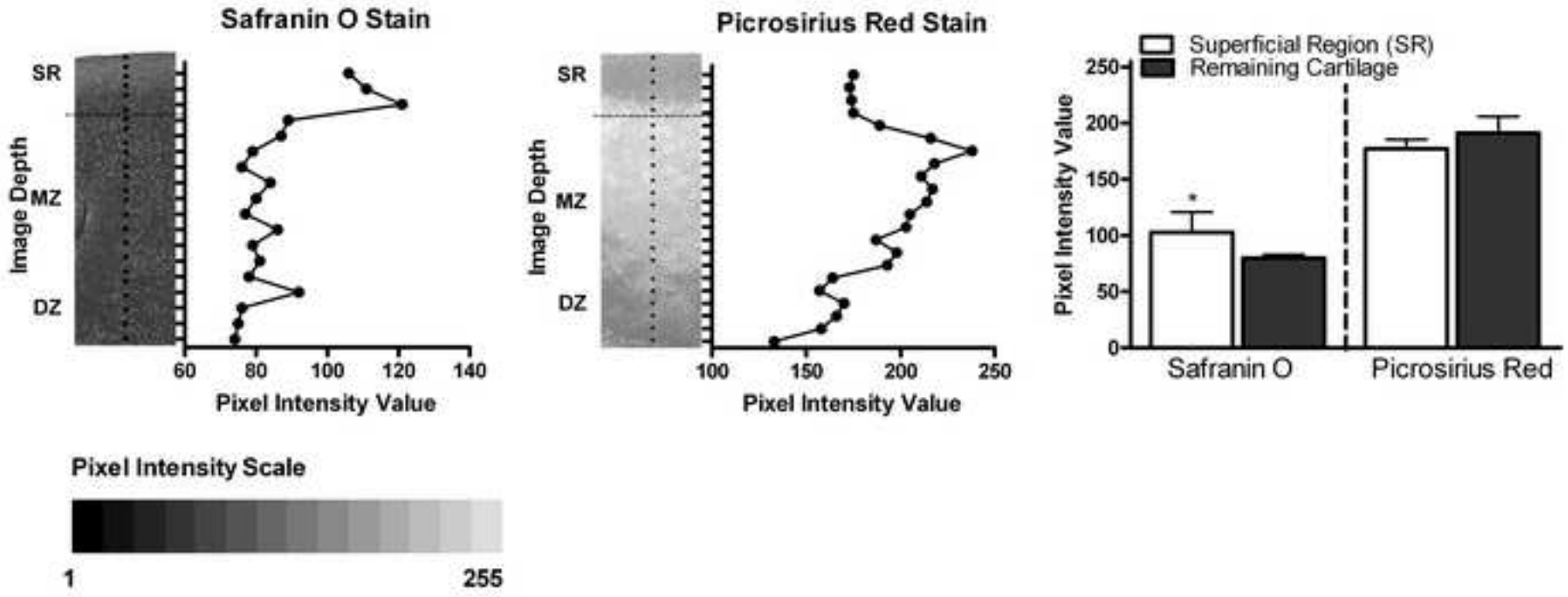

Figure 5

Click here to download high resolution image

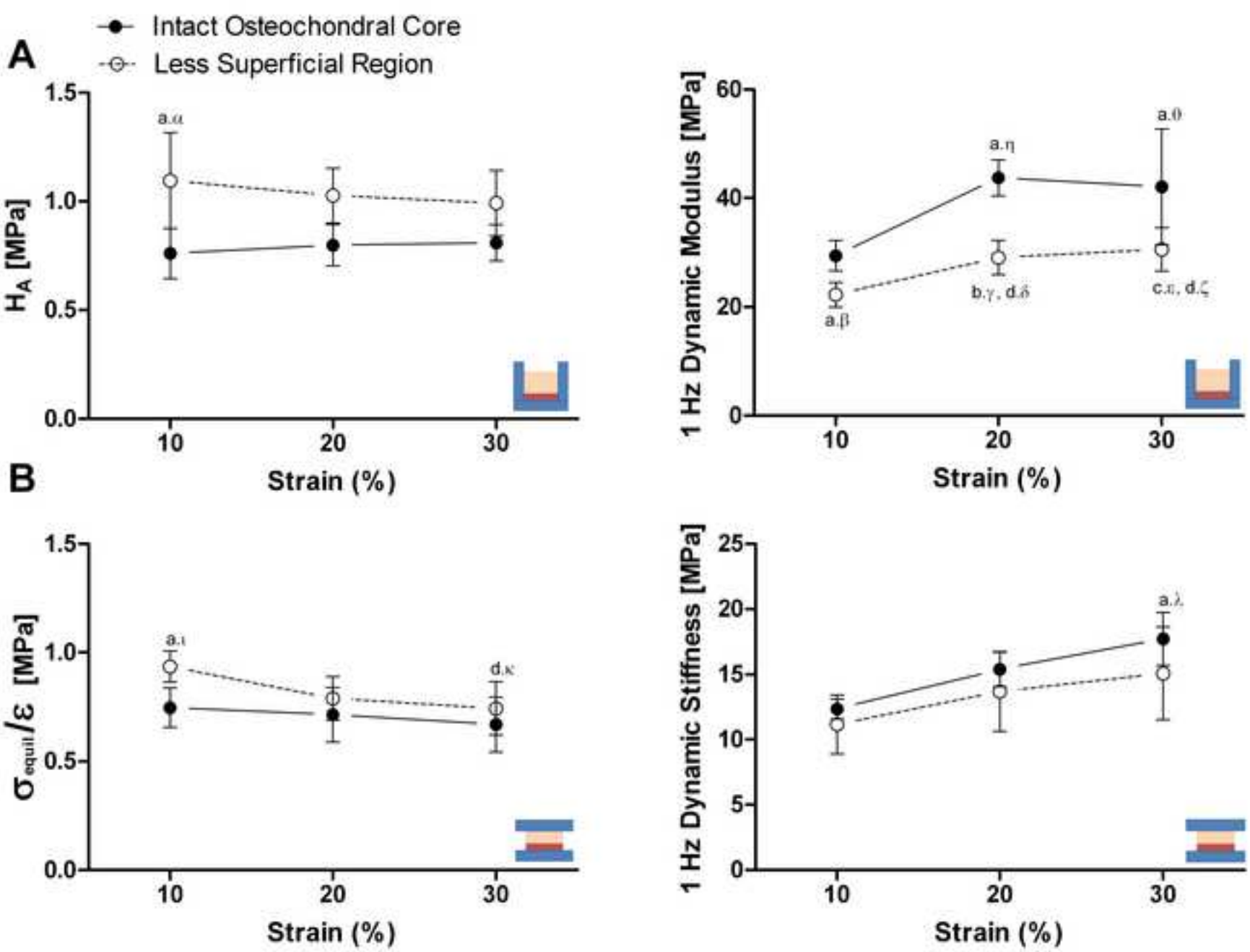

Figure 6
Click here to download high resolution image

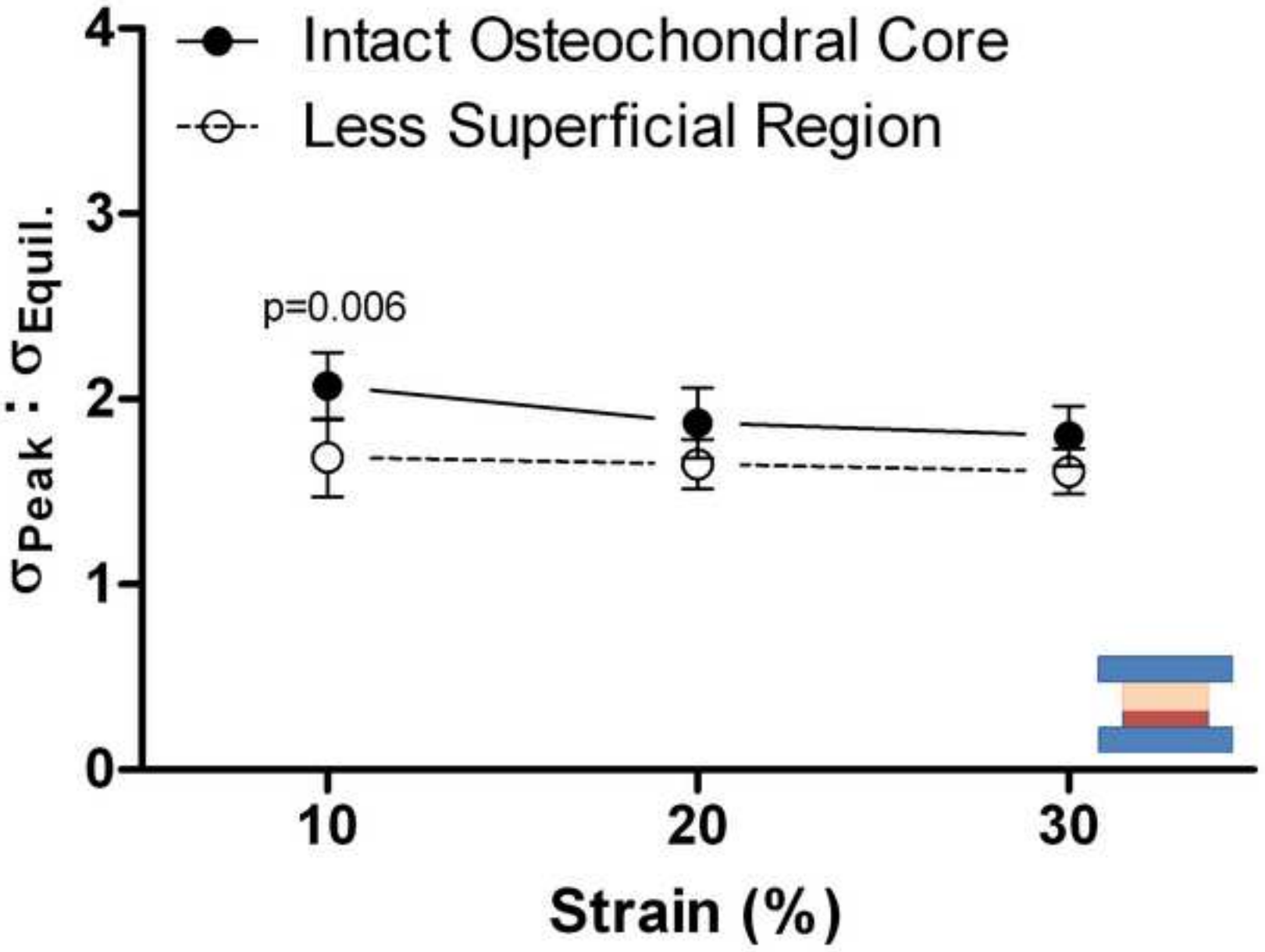

Figure 7

Click here to download high resolution image